Low-temperature Si and Si:Ge epitaxy by ultrahigh-vacuum/chemical vapor deposition: Process fundamentals

by B. S. Meyerson

This paper is an overview of work at the IBM Thomas J. Watson Research Center on the chemical and physical considerations underlying the development of a low-temperature chemical vapor deposition process, designated ultrahigh-vacuum/chemical vapor deposition (UHV/CVD). The origins of the rigorous vacuum and chemical purity requirements of the process are discussed. Operating in the range of 500°C, the process has made it possible to explore the use, in silicon-based devices and atomic-length-scale structures, of a number of metastable materials in the Si:Ge:B system. Also discussed is associated experimental work on the fabrication of high-speed heterojunction bipolar transistors and high-mobility two-dimensional hole-gas structures.

Introduction

The ultrahigh-vacuum/chemical vapor deposition (UHV/CVD) process [1–3] is a chemical vapor deposition process for which operating temperatures (in the range of

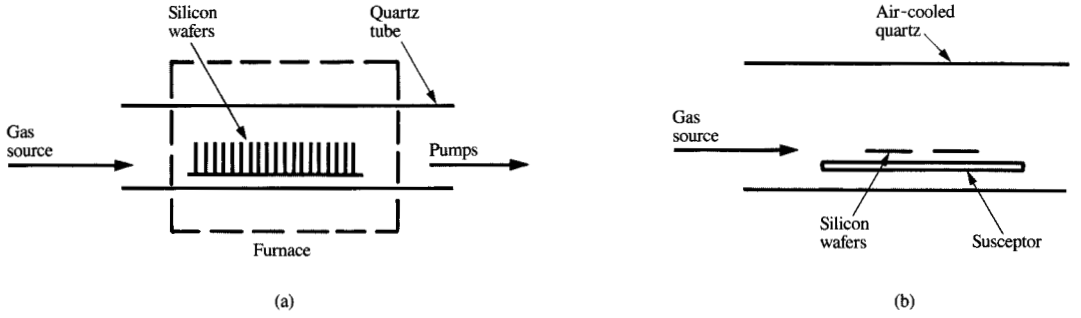

Figure 1

(a) Geometry of UHV/CVD reactor, showing high-density coaxial wafer placement; (b) geometry of conventional cold-walled epitaxy reactor.

500°C) are well below those associated with diffusive processes in silicon. It is predominantly by such processes, surface and bulk, that the silicon system restores itself to chemical and physical equilibrium. At temperatures at which the rates of such diffusive processes become negligible, limitations due to the solid solubility of a dopant species and/or the critical thickness of a strained Si:Ge epitaxial layer are greatly relaxed. This suppression of relaxation processes makes it possible to produce structures and devices of arbitrary Si:Ge and dopant compositions, with accurate control of composition on the atomic length scale. Employed in Si technology, this ability to customize the bandgap and doping of either bipolar or field-effect Si devices would offer the prospect of device performance heretofore restricted to devices based on III–V materials such as GaAs and GaAlAs. However, the challenges presented by the chemical attributes of the Si system are formidable.

Molecular beam epitaxy (MBE) has been the primary technique employed to prepare and study metastable materials in the Si system. Numerous studies of the fundamental properties of Si and its alloys [4–6] have led to advances in this field, but the fabrication of high-quality silicon devices has been found to be problematic using this technique. Recent studies [7, 8] have elaborated issues still to be resolved, the major ones being those related to the surface segregation of species such as Ge, Sb, and B. Such segregation is reduced or absent in the chemical vapor deposition of silicon at comparable processing temperatures, thereby offering the possibility of achieving improved dopant and alloy transitions.

Chemical aspects

In order to deposit silicon epitaxially onto a substrate, two fundamental conditions must be met. First, the initial growth interface must be atomically perfect and chemically pure, so that neither defects nor unintended impurities become incorporated into the resulting epitaxial layer. Second, the growth process must proceed in conditions of like purity, so that the controlled introduction of dopant species or species for the purpose of alloy formation is the sole process determining the final composition of a film. Furthermore, to take ultimate advantage of film composition control, one would wish to control composition on the scale of atomic lengths. This last goal is most easily attained at reduced film growth rates. As a consequence of this, the reactor geometry shown in part (a) of **Figure 1** was selected for implementing the UHV/CVD process. The placement of wafers is coaxial within a hot-walled furnace, in contrast to placement on a heated susceptor in conventional epitaxy, as indicated in part (b). A high wafer-packing density is thus achieved. Because the product of the number of wafers processed per run times the deposition rate can therefore be high, deposition rate considerations can be decoupled from process throughput considerations.

Fundamental in the development of any growth method are the development of associated techniques to control contamination, and, more specifically as applied to epitaxy, the development of techniques to control the contamination of the initial growth interface. That interface plays a critical role in an epitaxial growth process because it serves as a template for the layers to follow, and because associated, interfacial defects are replicated in the resultant layers. Furthermore, it integrates system contamination during the time preceding growth, thus leading to the introduction of impurities (boron being one example [9]) at levels that may be incompatible with subsequent device fabrication. In silicon epitaxy, the primary contaminating species encountered are oxides of

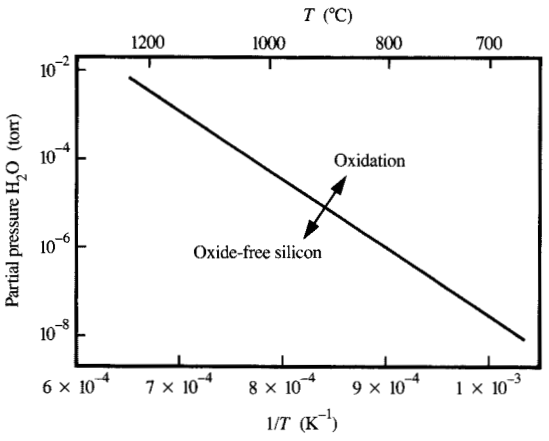

Figure 2

Extrapolation of the equilibrium data of Ghiddini and Smith [10, 11] for the formation of SiO_2 versus Si etching by SiO evaporation, shown as a function of H_2O partial pressure.

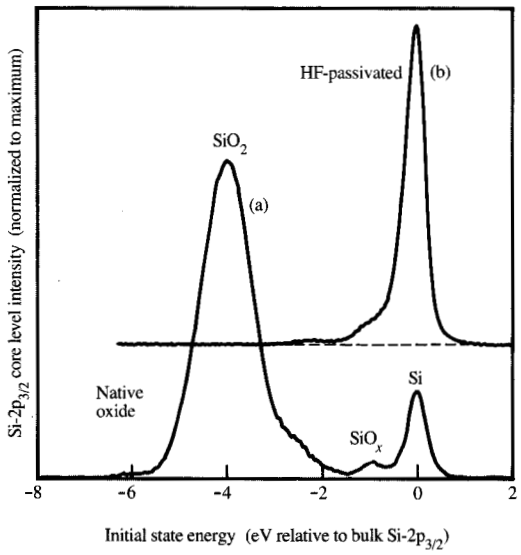

Figure 3

Photoemission spectra from the (111) surface of a Si wafer (a) as received, and (b) after HF-passivation and subsequent exposure to room ambient for ten minutes. From [13], reproduced with permission.

silicon. One must devise a means both for preparing an oxide-free silicon surface and for then maintaining it. To assess the difficulty of this task, we first consider those conditions under which Si oxidation can proceed.

Ghiddini and Smith performed several fundamental investigations [10, 11] of the oxidation reaction Si undergoes in the presence of two commonly occurring vacuum system contaminants, water vapor and oxygen. With regard to oxidation by reaction with water vapor, it was demonstrated that at high partial pressures of H_2O, a stable oxide is formed on the silicon surface by the reaction

$$Si(s) + 2H_2O \rightarrow SiO_2 + 2H_2 \uparrow .$$

However, at low partial pressures of H_2O, the silicon surface is etched because of the formation of the volatile suboxide SiO, viz.,

$$Si(s) + H_2O \rightarrow SiO \uparrow + H_2 \uparrow .$$

Ghiddini and Smith obtained data for the equilibrium condition, for which a crossover occurs from oxidation to etching, in the temperature range 900–1150°C. An extrapolation of their data downward in temperature is shown in **Figure 2**. The extrapolation indicates that in order to conduct epitaxy at temperatures significantly lower than 700°C, one must maintain the partial pressure of H_2O at ultrahigh-vacuum levels, as required for maintaining a bare Si surface. Similar requirements are found for the case of oxygen [10]. These data yield quantitative design points for the epitaxial growth of silicon, defining a "window" of operating conditions within which an oxide-free silicon surface would be maintained. It is important to note here that these conditions are taken from equilibrium data, and are thus applicable only to a static silicon surface in an oxidizing ambient. Under dynamic conditions, such as those applicable during actual film growth, there is a continuous flux of additional silicon to the growth surface, greatly reducing its sensitivity to oxidation. In such instances, oxygen is incorporated as a contaminant in the resultant layers, but is unlikely to disrupt film growth. Related to the question of how to maintain an oxide-free silicon surface is the question of how to prepare a silicon wafer with such an optimal surface and subsequently transfer it to a reactor without altering its state.

For simplicity it is preferable to start by producing an air-stable yet oxide-free silicon surface. This is achieved by employing a hydrogen-peroxide-based [12] chemical cleaning process, followed by a ten-second dip in 10:1 H_2O/HF. Terminating this sequence with a dip in HF results in the formation of a hydrophobic, air-stable, hydrogen-passivated silicon surface. The degree to which the surface is thus stabilized is remarkable, as demonstrated by the data shown in **Figure 3**. Spectrum (a) is composed of photoemission data taken from a wafer in an as-received condition. The dominance of the SiO_2 peak indicates that the formation of its native oxide is complete.

Spectrum (b) is composed of photoemission data taken after the treatment described above: H-passivated by an HF dip, and then allowed to remain in room ambient for ten minutes. As can be seen, there is no evidence of reoxidation, with the hydrogen adlayer acting as a chemical barrier to recontamination. One can estimate a 13-order-of-magnitude reduction in the reactivity of the silicon surface with respect to oxidation as a consequence of such hydrogen passivation. This ensures that silicon wafers prepared that way may be loaded into the UHV/CVD reactor through the ambient without oxidation and/or contamination of their surfaces. In contrast to other forms of low-temperature epitaxy by CVD [14, 15], no *in situ* cleaning step need be performed, as no native oxide exists at the inception of film growth. More quantitatively, secondary-ion mass spectrometry (SIMS) has shown there to be less than about one hundredth of a monolayer oxygen trapped at the initial growth interface at the completion of film deposition. Once the broad issue of contamination control has been addressed, basic issues of steady-state process chemistry and reactor hydrodynamics remain. Film-growth chemistry is considered in the context of two broad classes of chemical processes, those being homogeneous (gas-phase) and heterogeneous (gas/surface) chemical reactions.

In order to successfully deposit uniform and particle-free epitaxial silicon films in a high-density multiwafer processing geometry such as that in Figure 1(a), one must suppress homogeneous silane chemistry. Homogeneous chemistry in the silicon hydride system leads to the formation of the highly reactive intermediate silylene (SiH_2), which can insert into the parent silicon hydride, forming higher silanes. A simple example of this process is homogeneous silane pyrolysis, viz.,

$$SiH_4 \rightarrow SiH_2 + H_2 .$$

The reaction forms the highly reactive silylene radical, which can reinsert into the parent species by the reaction

$$SiH_4 + SiH_2 \rightarrow Si_2H_6 ,$$

or it can insert into Si–H bonds at a growth surface with near-unity efficiency. Species such as Si_2H_6 and SiH_2 which react efficiently with surfaces cannot transport into the high-aspect-ratio cavities existing between closely packed wafers, because the gaseous source is rapidly depleted of these species when they collide with surfaces. This leads to an excess of film growth at wafer edges, with the accompanying loss of film uniformity. This has been modeled and explicitly demonstrated for films grown directly from disilane [16] and for films grown in environments where disilane is formed *in situ* [17, 18]. In the extreme limit of high total pressure and high temperature, it is possible for the continued reinsertion of the silylene radical into parent hydrides to lead to the gas-phase nucleation of polymeric silicon hydride particulates, of the form $(SiH_2)_x$, rendering any resulting films useless because of associated high particle counts. The most direct approach one may take in avoiding any of these difficulties is to completely quench homogeneous silicon hydride reactions. To ensure uniformity in film growth, in addition to quenching the homogeneous reactions, one must also ensure the adequate diffusivity of the gaseous species to the growth interface such that depletion effects due to reactor hydrodynamics do not contribute to growth inhomogeneity. To address both the issue of homogeneous reaction suppression and that of reactor hydrodynamics, an operating pressure of 10^{-3} torr during film growth was chosen.

Nominally, the rate constant for the pyrolysis of a gaseous species such as silane is of the form

$$A \exp\left(\frac{E_a}{kT}\right) ,$$

where E_a is the activation energy of the process. In the limit of low total pressure P_T, referred to as the "falloff" regime, the prefactor A takes the form $A \propto P_T$, so that the rate constant falls off linearly with total pressure. This phenomenon was quantitatively described by Rice, Ramsperger, Kassel, and Marcus (RRKM), and the computational detail required to evaluate the effect is available in several texts [19, 20]. Put succinctly, the "falloff" of the rate constant with total pressure is a consequence of the decreasing rate of collisional energy transfer between molecules as the total pressure falls. The pressure below which the rate constant for the pyrolysis of a given species becomes linearly dependent upon pressure is a function of the efficiency of energy transfer between molecules, and the onset of this phenomenon for the case of silane occurs at 10 torr. Early workers studying silane pyrolysis, notably Purnell and Walsh [21], accounted for this phenomenon empirically by including a term $[SiH_4]^{1/2}$ in the prefactor of the rate constant expression. However, when RRKM-corrected, silane pyrolysis rates fall as shown in **Figure 4**. RRKM-corrected silane pyrolysis rate data are compared with an *invalid* extrapolation of the experimental data of Purnell and Walsh, downward in pressure. As is readily seen, operation of the UHV/CVD process at a pressure of 10^{-3} torr results in a large reduction in the rate constant for silane pyrolysis at a given temperature, and computation [22] shows that reactant depletion due to homogeneous pyrolysis at the operating conditions of interest is negligible as a consequence of this. A word of caution: This is not equivalent to the case in which highly dilute silane is employed at higher total pressures. Because the relevant parameter is total pressure, operation at the same partial pressure of silane, employing a high pressure of carrier

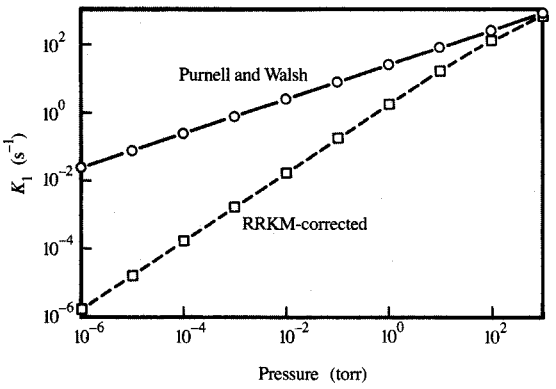

Figure 4

Reaction rates for silane pyrolysis, corrected according to the calculations of Rice et al. (see for example [19] and [20]). The rates are shown as a function of total pressure. For comparison, an extrapolation (downward in pressure) of the data of Purnell and Walsh [21] is included. From [22], reproduced with permission.

gas, is not an equivalent condition. Next, the impact on reactor hydrodynamics of operation at 10^{-3} torr is considered.

At a pressure of 10^{-3} torr, gas transport in the region of the wafer boat is by molecular flow, with the molecular mean free path (≃5–10 cm) significantly longer than typical interwafer or wafer/wall dimensions (≃1 cm). Operating in the molecular flow regime eliminates classical difficulties with high-pressure CVD methods, where the formation of boundary layers and/or recirculating flows leads to nonuniform film growth (usually resolved by mechanically complex wafer and/or gas-inlet motion) and makes the attainment of atomically abrupt compositional and doping transitions within the film a virtual impossibility. Furthermore, operation at this low pressure greatly reduces reactant residence times within the heated zone of the reactor, serving to minimize reactant depletion. In summary, low-pressure operation has thus been selected as the most straightforward approach to the attainment of a high degree of film uniformity in the geometry selected for the UHV/CVD process. The net effect of this choice of processing conditions is that film growth proceeds by the heterogeneous pyrolysis of the gaseous source species that

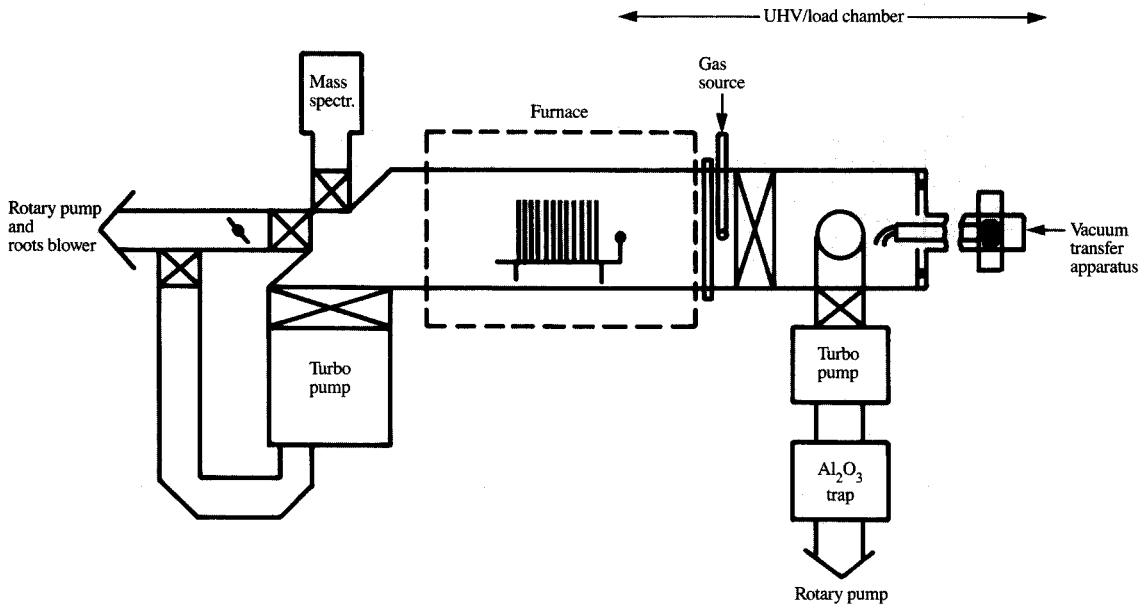

Figure 5

Schematic of UHV/CVD system. From [1], reproduced with permission.

are employed: silane (SiH_4), germane (GeH_4), diborane (B_2H_6), and phosphine (PH_3).

Film growth

A schematic of the UHV/CVD system used for the work described subsequently is shown in **Figure 5**. Typically, wafers are first RCA-cleaned, and then subjected to a 10:1 H_2O/HF dip for ten seconds. They are then placed coaxially in a wafer boat holding at maximum 35 wafers, and the boat is placed within the system load-lock. The load chamber is held at approximately 100°C while being evacuated to below 10^{-6} torr, and the wafers are then transferred under flowing hydrogen into the UHV portion of the system. The flow of gaseous source species is then commenced within a time during which the hydrogen surface passivation created by the HF dip is maintained, five minutes being typical.

At nominal growth conditions, 10^{-3} torr at 550°C, chemical processes important to film growth, such as dopant and germanium incorporation, are linear in gaseous content and are thus readily controlled. An example of boron profile control that is possible is seen in **Figure 6**. Discrete concentration steps over a narrow dopant range are readily achieved because dopant content depends linearly on dopant flow. This is in marked contrast to beam deposition techniques such as MBE, where reactant fluxes to surfaces are exponential in source temperature, as is dopant incorporation, making precision concentration control difficult. In the present process, dopant incorporation and Ge alloy formation are all found to be strong functions of the deposition temperature. However, it is straightforward to control reactor temperatures to within several tenths of a degree, so that film composition is controlled with precision over a wide dynamic range solely by the composition of the gaseous source employed. Film thickness is linear in time, as expected, and thus can be controlled with a precision determined by the chosen growth rate. The growth conditions above yield a growth rate of approximately 3 Å/min for intrinsic or boron-doped silicon epilayers. This value has been found to be suitable for the devices discussed subsequently, but can be varied widely if required for the growth of thicker layers. Values can be widely varied because the growth rates are thermally activated with an activation energy of ~1.6 eV. The growth of Si:Ge alloy films reveals a more complex behavior; a cooperative growth phenomenon is encountered. The addition of germane to the silane source results in the behavior seen in **Figure 7**, where growth rates are strongly enhanced by the presence of germane. It is seen that germane greatly enhances the efficiency of the growth, accelerating it by a factor of about 25 for films containing about 20 percent germanium. Thus, the reaction efficiency of silane is enhanced considerably by the presence of germane. The dashed line in the figure

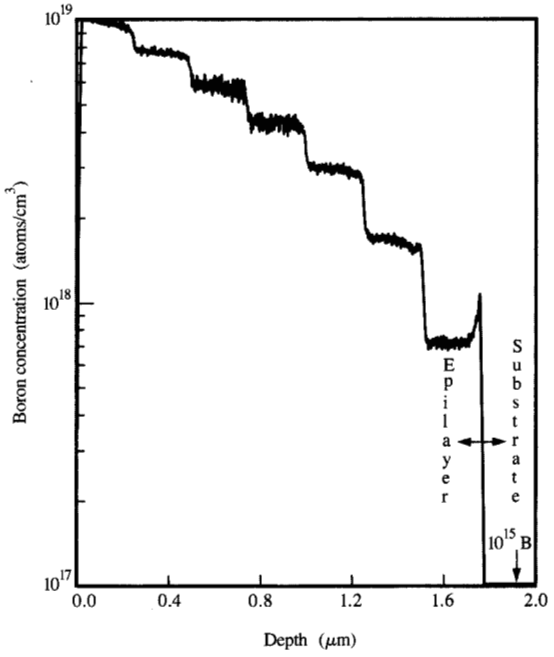

Figure 6

SIMS data for a stepwise profile of boron in silicon, illustrating the boron-profile control that can be achieved with the UHV/CVD process. From [1], reproduced with permission.

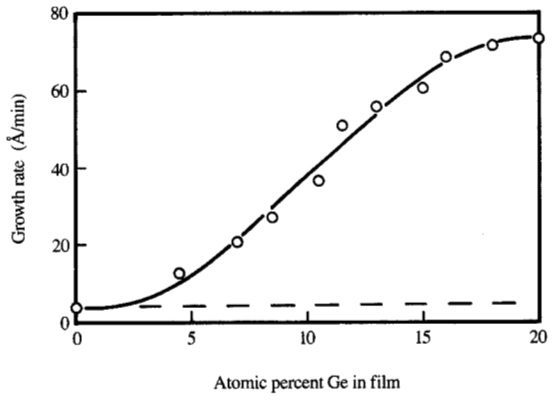

Figure 7

Film growth rate as a function of Ge content in a Si:Ge alloy film. From [3], reproduced with permission.

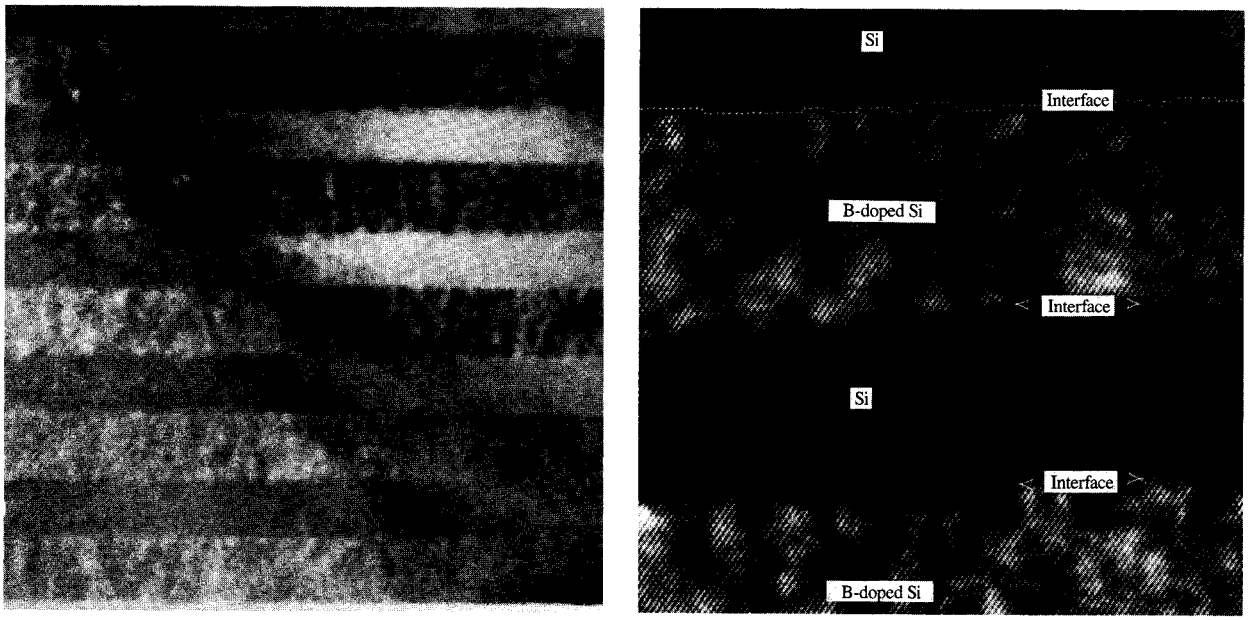

Figure 8

Cross-sectional TEM micrographs of a Si/Si:B dopant superlattice. The superlattice in (a) has been lattice-imaged in (b), with a delineated "interface," added for identification purposes.

provides a reference for the case in which growth rates are additive, as seen for boron as an example. The origins of the enhancement have been discussed in detail elsewhere [3]. Briefly, it was shown that the presence of germanium on the growth surface reduces the energy required for hydrogen desorption relative to its value for desorption from pure silicon. Chemical vapor deposition under the conditions used in the UHV/CVD process has been modeled to be rate-limited by hydrogen desorption, and any phenomenon accelerating that process results in more rapid film growth. Although this effect complicates the attainment of controlled Ge profiles, it has been overcome, as will be demonstrated.

Materials

The combined effect of employing a relatively low growth temperature, short system residence times, and relatively slow growth rates makes it possible to obtain extraordinarily abrupt transitions in both dopant content and/or alloy composition. In addition, the use of such growth temperatures has made it possible to deposit high-quality layers of nonequilibrium materials, for example, as can be seen in **Figure 8**. The figure contains cross-sectional TEM micrographs of a dopant superlattice in the Si:B materials system. The superlattice comprises alternating layers of intrinsic Si and Si:B alloy containing 10% B (5×10^{21} boron atoms/cm^3), with all layers fully commensurate and free of precipitates. The layers containing boron are highly strained, and the contrast visible in the micrographs is taken to be primarily a consequence thereof. Each layer is roughly 40 atoms thick. This structure is an extreme example of metastable material fabrication by the UHV/CVD process. The upper bound on substitutional boron content in silicon is 2×10^{20} boron atoms/cm^3, approaching this value at temperatures in excess of 1100°C. At the growth temperature employed, 550°C, boron incorporation exceeds the equilibrium value by approximately three orders of magnitude. Annealing at 900°C for several minutes suffices to return the sample to equilibrium, as large precipitates form, and the silicon lattice is disrupted. However, the layers are quite stable at temperatures below 700°C, and can be employed in devices as highly degenerate contacts or single-crystal emitters. It is found that such layers are highly conductive as deposited, with measured conductivities corresponding to carrier densities of 1.5×10^{20} cm^{-3}. Hall measurements reveal a higher degree of activation (×2) with a degraded mobility. Attaining high conductivities without a high-temperature dopant activation step creates the unique opportunity to fabricate devices whose dimensions are determined solely by the accuracy of deposition process control, rather than by postprocessing-induced diffusion. This takes us to the next matter one must address: process/material control.

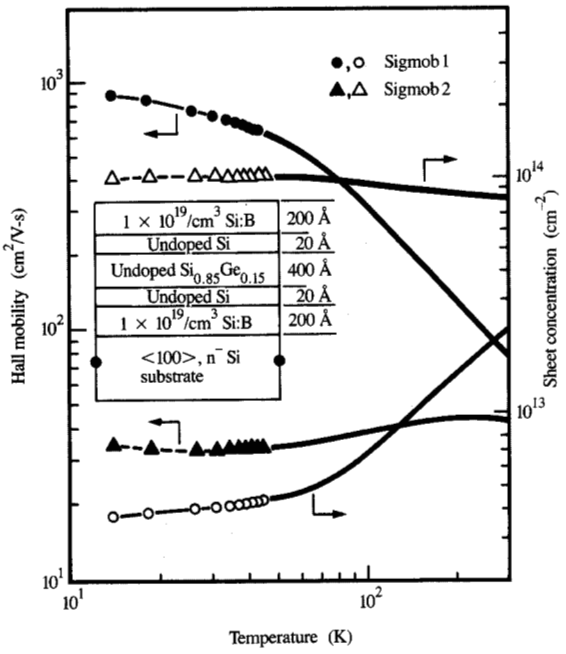

Figure 9

Hall-mobility and carrier-density data for two symmetrical two-dimensional hole-gas (2DHG) heterostructures that were fabricated. A schematic of the cross section of one of them (Sigmob1) is included. The other heterostructure (Sigmob2) had the same cross section but was boron-doped throughout. As expected, Sigmob2 did not exhibit mobility enhancement.

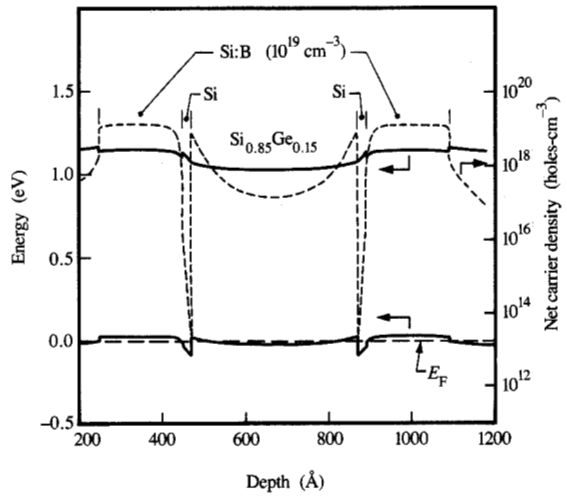

Figure 10

Energy-band diagram for the heterostructure Sigmob1.

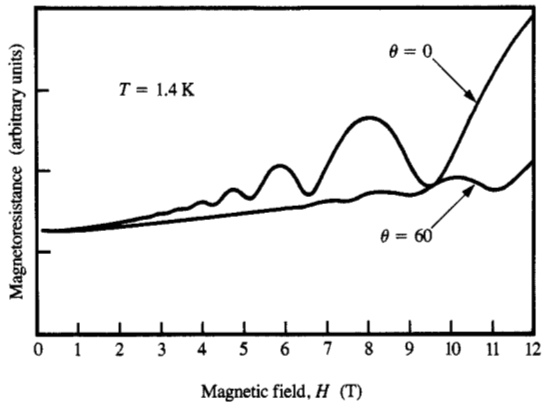

Figure 11

Schubnikov–de Haas magnetoresistance data obtained from the symmetrical two-dimensional hole gas generated in the heterostructure Sigmob1. From [23], reproduced with permission.

If ideal, the control of film composition should be absolute from the perspective of concentration and location. Transitions between regions of varying alloy composition, as well as between regions of differing dopant content, should be atomically abrupt. Conventional analytic methods lack the required precision and sensitivity to determine this in a quantitative fashion, so the measurement of electronic properties of films was used to investigate compositional transitions.

A two-dimensional hole-gas (2DHG) structure, designated as *Sigmob1*, was deposited by UHV/CVD. A schematic of the structure and associated Hall-effect data are shown in **Figure 9**. For reference, also shown are data for *Sigmob2*, which was uniformly doped across all of its layers, thus failing to exhibit enhanced mobility at low temperature. The band structure of Sigmob1 is shown in **Figure 10**. Two hole gases are formed (shown for $T = 77$ K), one each at the Si/Si:Ge and Si:Ge/Si transitions, each centered at a depth of 10–20 Å into the Si:Ge well. These gases serve as extraordinarily sensitive probes of the abruptness of the boron-dopant and Si:Ge alloy transitions because they are less than ten atomic layers removed from the boron-doped Si layers. The uncontrolled incorporation of residual boron into the Si:Ge well region would greatly degrade the mobility of holes in the well. Furthermore, as growth proceeds, the first interface forms moments after the cessation of intentional boron incorporation, while the

second interface forms significantly later. The extent to which the hole gases formed at the interfaces are identical is thus a highly sensitive measure of the abruptness of dopant transitions. If there were a significant chemical memory in the system, such that the boron content in the films decayed gradually at the first transition, the hole gas formed at the first interface would be of higher density and lower mobility than that at the second. Schubnikov–de Haas (SdH) data were employed [23] to explore this possibility, and are shown in **Figure 11**. The data are remarkable in that a single set of oscillations is seen in the magnetoresistance of the layers. The onset of oscillations in a SdH measurement occurs when $\mu H > 1$. The two hole gases formed each produce an independent set of oscillations. The exact alignment of these oscillations, producing the single peaks in Figure 11, indicates virtually identical mobility and carrier density at the two interfaces, and demonstrates that abrupt boron transitions were obtained. In order to verify that two hole gases were indeed formed, carrier densities were calculated from the SdH data. The calculated densities were half those measured by Hall-effect methods, the expected result because Hall measurements probe the total carrier population, while SdH data reflect the properties of each gas independently. This demonstrated that a buffer width of 20 Å was sufficient for the transition from the heavily doped Si region to the intrinsic Si:Ge carrier well. TEM observation of the alloy transitions was consistent with this, showing the Si/Si:Ge alloy transitions to be both abrupt and defect-free in the limit of the TEM method. The record high-mobility/carrier density product [24] seen for this sample also indicates the quality of the layers.

Devices

Device properties are critically dependent upon many aspects of the material preparation method which cannot be readily tested by other means. Issues such as process reproducibility, particle counts, growth rate uniformity across a wafer and wafer-to-wafer, and compositional control within a wafer and wafer-to-wafer are all critical in the processing of devices, and cannot be ignored when working toward the development of a technologically useful materials system.

In our device work, the UHV/CVD process has been employed exclusively for the fabrication of "epi-active" [25] devices, defined as devices for which critical high-field regions of the device reside in the deposited material. Additionally, a significant number of growth and processing interfaces lie within the active regions of such a device. This requires that those interfaces be free of contamination and damage generally resulting from high-energy processes (e.g., reactive ion etching) employed in device and circuit fabrication. The UHV/CVD process has been used to fabricate a wide variety of epi-active devices, both homojunction [26–28] and heterojunction [29–31] bipolar transistors. The devices make use of the control inherent in the UHV/CVD process to deposit epitaxial semiconductor layers only several hundred angstroms thick, on patterned substrates, with complex overlapping dopant and alloy profiles. By means of the process, it has been possible to tailor the band structure of a bipolar transistor to incorporate (by virtue of the tailored band structure) a built-in accelerating field across its base. Recently, Patton et al. [30] have used the process to fabricate a series of Si:Ge-based heterojunction bipolar transistors having such graded base profiles. They set new device speed records for both homojunction and heterojunction bipolar transistors, displaying unity gain cutoff frequencies F_T of 52 GHz and 75 GHz, respectively. Devices ranging in area from 1–10 000 μm^2 showed ideal behavior—a remarkable result when one considers that the Si:Ge devices were fabricated using a materials system that is highly strained, and thus metastable. Although the device fabrication procedure involved annealing for 20 minutes at 850°C, the metastable structures survived. These results point out a rich area for further research into identifying the true stability limits and defect nucleation mechanisms active in the Si:Ge materials system.

Concluding remarks

To look to the future in this field of research, it is necessary to examine its origins. This work was driven by an interest in developing a chemical vapor deposition process for preparing metastable silicon-based layers in a manner that prevented their relaxation to a ground state. That goal has been met, leading to the formation of new metastable silicon alloys with compositions well outside previously accepted ranges. For example, the Si:B alloy containing 10% boron is a truly unique material whose boron content far exceeds any postulated value, independent of preparation temperature. Equally interesting is the remarkable stability of the Si:Ge layers that have been prepared. Although a large body of literature has been devoted to concepts such as the critical thickness of Si:Ge layers, little work has been performed exploring the fundamental mechanisms of the relaxation process in such layers. Recent work [32] has shown that compositionally identical Si:Ge superlattices, upon annealing, may either fail by catastrophic defect nucleation and multiplication, or may simply interdiffuse without the formation of extended defects. It was found that the condition of the interfaces of the superlattices was critical to the relaxation path that was taken; highly perfect interfaces were found to preclude defect nucleation. Certainly, the continued study of the kinetics of relaxation in such layers will be necessary if they are to be utilized in future semiconductor devices.

References

1. B. S. Meyerson, *Appl. Phys. Lett.* **48**, 797 (1986).
2. B. S. Meyerson, F. K. LeGoues, T. N. Nguyen, and D. L. Harame, *Appl. Phys. Lett.* **50**, 113 (1987).
3. B. S. Meyerson, K. J. Uram, and F. K. LeGoues, *Appl. Phys. Lett.* **53**, 2555 (1988).
4. S. Iyer, R. A. Metzger, and F. G. Allener, *J. Appl. Phys.* **52**, 5608 (1981).
5. R. People, *Phys. Rev. B* **32**, 1405 (1985).
6. D. V. Lang, R. People, J. C. Bean, and A. M. Sergent, *Appl. Phys. Lett.* **47**, 1333 (1985).
7. D. J. Eaglesham, H. J. Gossman, and M. Cerullo, *Phys. Rev. Lett.* **65**, 1227 (1990).
8. S. S. Iyer, J. C. Tsang, M. W. Copel, P. R. Pukite, and R. M. Tromp, *Appl. Phys. Lett.* **54**, 219 (1989).
9. S. S. Iyer, S. L. Delage, and G. J. Scilla, *Appl. Phys. Lett.* **52**, 486 (1988).
10. F. W. Smith and G. Ghiddini, *J. Electrochem. Soc.* **133**, 1300 (1982).
11. G. Ghiddini and F. W. Smith, *J. Electrochem. Soc.* **131**, 2924 (1984).
12. W. Kern and D. A. Puotinen, *RCA Rev.* **31**, 187 (1970).
13. B. S. Meyerson, F. Himpsel, and J. K. Uram, *Appl. Phys. Lett.* **57**, 1034 (1990).
14. T. Ohmi, T. Ichikawa, T. Shibata, K. Matsudo, and H. Iwabuchi, *Appl. Phys. Lett.* **53**, 45 (1988).
15. T. J. Donahue and R. Reif, *J. Appl. Phys.* **57**, 2757 (1985).
16. B. S. Meyerson, B. A. Scott, and R. Tseui, *Chemtronics* **1**, 166 (1986).
17. B. S. Meyerson and W. L. Olbricht, *J. Electrochem. Soc.* **131**, 2361 (1984).
18. B. S. Meyerson and J. M. Yu, *J. Electrochem. Soc.* **131**, 2366 (1984).
19. J. Robinson and K. A. Holbrook, *Unimolecular Reactions*, Wiley Interscience Press, New York, 1972.
20. W. Forst, *Theory of Unimolecular Reactions*, Academic Press, Inc., New York, 1973.
21. J. H. Purnell and R. Walsh, *Proc. Roy. Soc. A* **293**, 543 (1966).
22. B. S. Meyerson and J. M. Jasinski, *Appl. Phys. Lett.* **61**, 785 (1987).
23. P. J. Wang, F. F. Fang, B. S. Meyerson, J. Nocera, and B. Parker, *Appl. Phys. Lett.* **54**, 2701 (1989).
24. P. J. Wang, B. S. Meyerson, F. F. Fang, J. Nocera, and B. Parker, *Appl. Phys. Lett.* **55**, 2333 (1989).
25. G. L. Patton, D. L. Harame, G. J. Scilla, F. K. LeGoues, E. Ganin, P. J. Wang, and E. F. Crabbe, *Proc. Sixth Int. Symp. Silicon Mater. Sci. & Technol.* **90-7**, 174 (1990).
26. T. Nguyen, D. L. Harame, J. M. Stork, F. K. LeGoues, and B. S. Meyerson, *Technical Digest, Proceedings of IEDM '86*, IEEE, Los Angeles, 1986, p. 304.
27. J. M. Stork, D. L. Harame, B. S. Meyerson, and T. Nguyen, *IEEE Trans. Electron Devices* **36**, 1503 (1989).
28. H. Harame, J. M. Stork, B. S. Meyerson, T. N. Nguyen, and G. J. Scilla, *Electron Device Lett.* **10**, 156 (1989).
29. G. L. Patton, D. L. Harame, J. M. Stork, B. S. Meyerson, G. J. Scilla, and E. Ganin, *Technical Digest, 1989 Symposium on VLSI Technology*, IEEE, Kyoto, Japan, 1989, p. 95.
30. G. L. Patton, J. H. Comfort, B. S. Meyerson, E. F. Crabbe, G. J. Scilla, E. DeFresart, J. M. Stork, J. Y. Sun, D. L. Harame, and J. Burghartz, *Electron Device Lett.* **11**, 171 (1990).
31. G. L. Patton, D. L. Harame, J. M. Stork, B. S. Meyerson, G. J. Scilla, and E. Ganin, *Electron Device Lett.* **10**, 534 (1989).
32. S. S. Iyer and F. K. LeGoues, *J. Appl. Phys.* **65**, 4693 (1989).

Received June 21, 1990; accepted for publication December 11, 1990

Bernard S. Meyerson *IBM Research Division, Thomas J. Watson Research Center, P.O. Box 218, Yorktown Heights, New York 10598.*

Dr. Meyerson received a Ph.D. in physics from the City College of the City University of New York in 1981. He subsequently joined the IBM Thomas J. Watson Research Center as a Research Staff Member. Initially he worked on amorphous semiconductors, primarily diamondlike (hydrogenated amorphous) carbon films, investigating their electronic properties as related to local atomic ordering. In a broadening of that effort, the tribological properties of such films are currently being investigated, and he has organized several conferences pertaining to them. Recently, his work has been in the field of low-temperature epitaxy, demonstrating unique materials and devices in a number of metastable materials systems (Si–Ge, Si–B, and Si–Ge–B alloys). At present he manages the Electronic Materials group within the Physical Sciences Department, and is continuing his studies in the field of heteroepitaxy. Dr. Meyerson received the Young Authors Award from the American Association of Crystal Growth in 1987 for developing the ultrahigh-vacuum/chemical vapor deposition (UHV/CVD) process.